J Nanostruct 15(4): 1700-1709, Autumn 2025

RESEARCH PAPER

Graphite Nanosheet Prepared by Nickel Sulfate Exfoliating and Thermal Treatment and Its Action in Photodegradation of Crystal Violet

Eman Turky Shamkhy [1], *Amjed Mirza Oda* [2] *

[1] *Department of Basic Science, College of Dentistry, University of Baghdad, Iraq*

[2] *Science Department, College of Basic Education, University of Babylon, Babylon, Iraq*

ARTICLE INFO

Article History:
Received 06 June 2025
Accepted 03 August 2025
Published 01 October 2025

Keywords:
Crystal violate dye
Nanographite
Nanosheet
Nickel sulfate
Photodegradation

ABSTRACT

Nanographite surface was prepared by heat treatment of graphite-saturated nickel sulfate as an exfoliating agent to produce a very fine brown powder. The procedure depends on heating the saturated sample and oxidation by 50% of nitric acid with ultrasonic bath. The resulting powder is easily dispersed in water and characterized by UV-vis spectroscopy, where the new absorption at 224 nm is not present in bulk graphite and reveals of formation of oxidized nanographite. FTIR showed the skeleton of graphite is changed and new absorption of C=O. XRD of highly crystallized graphite modified to low-intensity peak as an indication of sheets displacement. SEM image showed the microscale flake of nanographite as singular flakes with different dimensions. Photocatalysis reaction was done for crystal violate dye in aqueous solution combined with UV lamp. The nanosheets have the ability for photodegradation of CV lasted 180 min but in the presence of H_2O_2, the vanishing needs 15 min with 96% photodegradation efficiency.

How to cite this article
Shamkhy E., Oda A. Graphite Nanosheet Prepared by Nickel Sulfate Exfoliating and Thermal Treatment and Its Action in Photodegradation of Crystal Violet. J Nanostruct, 2025; 15(4):1700-1709. DOI: 10.22052/JNS.2025.04.018

INTRODUCTION

Graphite is a widely distributed mineral usually present in metamorphic and igneous rocks, where its structure has the hyperdization sp^2p_z of p-electrons for carbon atoms [1]. This mineral feature is a layer of soft slices and the specific gravity is very low [2]. Graphite is an excellent thermal and electrical conductor with high regular stiffness and strength [3]. The stiffness and strength of graphite can be maintained at temperatures exceeding 3600 °C [2]. It's a highly lubricating, chemically inert, and corrosion-resistant substance [4]. These unique characteristics allow for wide and variant applications. Graphite can be classified into two types: the natural ones in the land and synthetic ones like wood processing. Three types of natural graphite [5], crystalline (flake graphite), lump graphite, and amorphous graphite the physical and chemical properties are different for each one another [2], owing to differences in precursor materials and graphite formation processes [6]. Graphite's inherent features like electrical conductivity is high, absorbance of light very low, also it has chemical resistance. These significant features made this material state-of-the-art application, such as medical implants and flexible

* *Corresponding Author Email: Almajid1981@gmail.com*

electronic devices.

Graphene is a nanosheet that can be synthesized from its precursor graphite depending on physical or chemical roots. Some techniques are very effective like different chlorate oxidants and permanganate can be used to synthesize graphene oxide (GO) from graphite [7, 8].

The Hummers' approach, [9, 10] in which the oxidation of graphite is processed by KMnO4 with aiding of strong acid treatment, is now the most widely used method for synthesizing GO. As a comparison to graphite, the spacing base is wider in GO. The presence of oxygenated groups in the parallel carbon layers causes a widening gap. Furthermore, chemical and thermal, and microwave-assisted treatment can be utilized to reduce GO, where the procedure and starting material significantly influence the final properties of graphene [10, 11].

Since Novoselov and Geim isolated graphene using Scotch tape in 2004, other methods for preparing graphene sheets have been devised [12]. For example, chemical vapor deposition [13] and epitaxial growth [14, 15], produce graphene with a low defect count, making these processes attractive for use in electrical devices [16]. These surface-based approaches, on the other hand, do not scale well for applications that require large amounts of graphene. By physically and chemically exfoliating bulk graphite, far more graphene can be created [17]. These sheets are useful in photocatalytic reactions like g-C_3N_4 (graphite-carbon nitride). These have 2D and high stability and also a high specific area with high existent of active groups [18]. graphite oxide nanosheets were prepared by ethylene glycol passivation as reported. The prepared material was very stable and used for the photocatalytic reaction for methyl orange degradation [19].

In this paper, we introduce the formation of nanographite by impregnation with nickel sulfate to make metal intercalation then heating is applied for exfoliating and this process is supported by characterization by UV-vis analysis, FTIR, XRD, and SEM to evaluate the conformation of graphite to nanographite. This nanosheet was examined in the photodegradation of crystal violate as a new material for the decantimination of wastewater. By studying the effect of reaction time, weight of nanographite, and addition of hydrogen peroxide to evaluate and get satisfying photodegradation of CV.

MATERIALS AND METHODS

Materials

Nickel sulfate heptahydrate (Fluka), graphite (Merck), HNO_3 (GCC), and ethanol (Thompson Baker).

Instrumentation

Water is used as a blank in UV-vis spectroscopy (Jenway spectrometer model 6800) with quartz cuvettes. With the KBr disk approach, the FTIR instrument (Affinity IR instrument, Shimadzu, Japan) recorded in the 400–4000 cm−1 range, and the XRD apparatus (DX-2700 SSC 40 kV/30 mA,

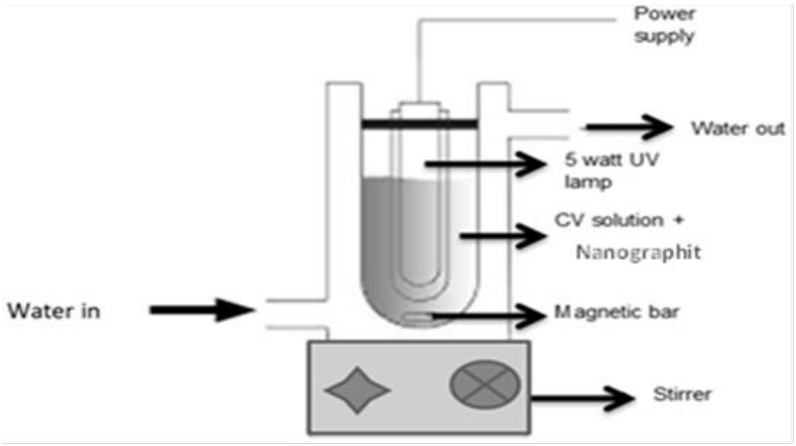

Fig. 1. Schematic photoreactor is used for CV photodegradation by nanographite.

USA) tested in the 20–80 (2θ) range. The scanning electron microscope Inspect 550, Netherlands, which operates at 25 kV, is used to perform SEM test. Ultrasonic bath model LTUSB by Labtech, Korea. Labtech muffle furnace for the heating process.

Procedure

Preparation of nanogrphite

To prepare the nanographite, the procedure was: 2.5 g of nickel sulfate heptahydrate dissolved in 150 ml distilled water in a beaker with a capacity of 250 ml subsequently combined with 2 grams of graphite powder, and for two hours, the group was stirred. The graphite was saturated with nickel sulphate and then the solution was filtered and the precipitate was dried at 60 c for 8 hours. 1 g of the mixture was put into the ceramic crucible and heated to 500 C° for two hours. After cooling at room temperature, 0.5 g was taken in a 100 ml beaker and 50 ml of HNO3 (50%) was added and stirred for a half-hour the solution was diluted with distilled water, and the slurry was separated by the centrifuge and washed with distilled water several times to get rid of excess acid. The collected suspension was added to a beaker containing 50 ml distilled water and put in the ultrasonic water bath for 20 minutes then the solution was left to stagnate and the brown colloidal was collected from upper solution by decantation and then the decanted solution was centrifuged and washed with ethanol 3 times. Then the brown powder is dried at 80 c for 6 hours so the sample is ready for characterization using scanning electron microscopy (SEM), UV-vis spectroscopy, Fourier transform infrared (FTIR), and x-ray diffraction (XRD). copper tube Cu (Cu Kα, λ = 0.15406 nm) with an XRD apparatus (DX-2700 SSC 40 kV/30 mA).

Photocatalysis experiments

All experiments of photodegradation of CV dye by nanographite were done in the immersion reactor as in t. The reactor is a glass tube with aiding of water cooling and a 5 W lamp cover with a glass tube immersed in the CV solution. The preliminary experiment was donedone by weigh 0.02 gm of nanographite and addingg to 10 ppm of CV solution with mixing on a magnatic stirrer for 30 min for adsorption equilibrium (at pH=7 and room temperature). After that, the lamp turns on and 2 mL of suspension is drawn after regular time. The photodegradation of CV dye is examined by measuring the absorbance at 590 nm. The effect of nanographite was studied by varying the weight in the range of 0.01-0.04 gm and applying the above procedure. Also, the effect of hydrogen peroxide was studied in the concentration range 0- 4*10-5 M. To calculate the photodegradation efficiency %; of CV in the interval time depending on the initial concentration (C_0) of CV and the concentration after illumination (C); by using the equation:

photodegradation efficiency %= $[(C_0-C)/ C_0]* 100$

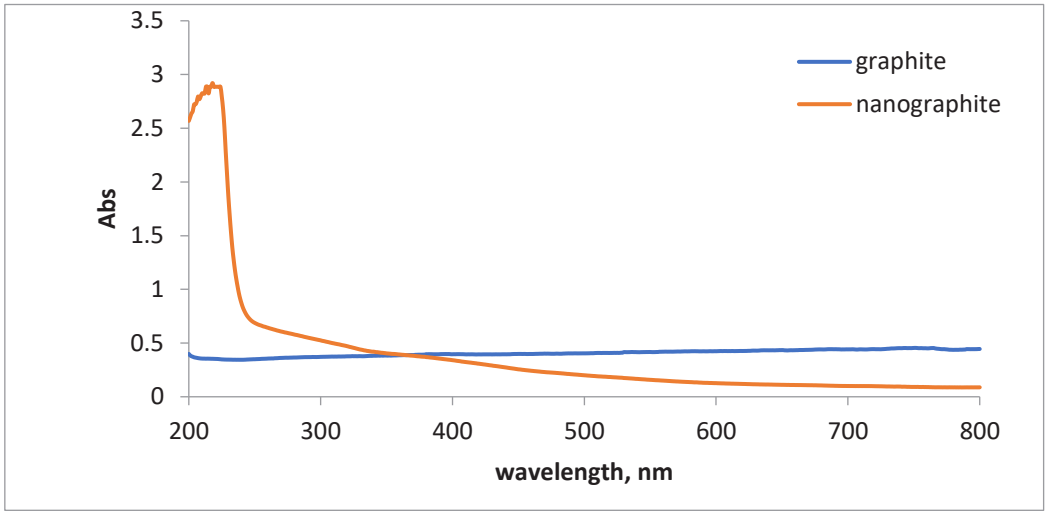

Fig. 2. The UV-vis spectrum of the graphite and nanographite.

RESULTS AND DISCUSSION

The effect of nickel sulfate salt on the structural properties of graphite was studied through the process of immersing them in water to get saturated graphite with solvated ions and then exposing the heating process. It was observed that the color of graphite turned into a brown color easily distributed in the water. The uv-vis spectrum of the nanographite solution was measured within the range 200-800 nm, where it is observed through the absorption spectrum that graphite does not have a specific absorption peak within the measured range, while the nanographite appeared to have a sharp absorption peak at 224 nm belong to the transition of electrons within π- π* resulting from the double bonds in the nanographite. Weak absorptions at 280-300 nm resulting from absorption of the n- π* type and as a result of the formation of C-O bonds within the graphite ring is a sign of the occurrence of layer displacement from each other to form nanographite. The third transition around 300-350 nm is due to the trapping of excited-state energy by the surface [20]. Also, there is no absorption of the pristine graphite where there is no distinct peak as shown in Fig. 2, which shows the uv-vis spectrum of the graphite and nanographite.

FTIR was measured for graphite, graphite-nickel

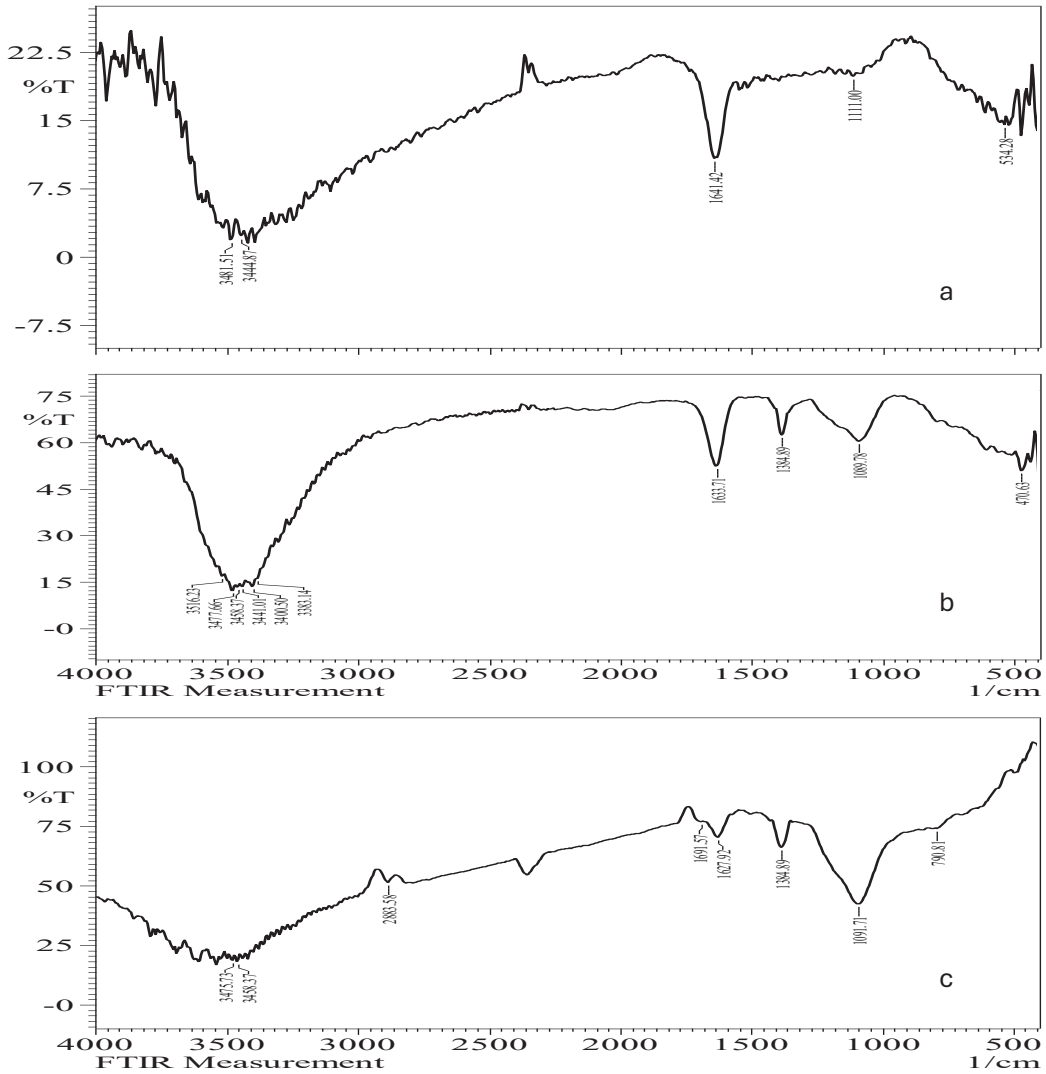

Fig. 3. FTIR of graphite (a), treated graphite with nickel sulfate (b), and purified nanographite (c).

sulfate after heating, and nanographite after purification Fig. 3, where O–H stretching vibration (3420 cm^{-1} is due to water adsorption. The peaks vibrational band at 1641 corresponding to C=C, vC=O stretching at 1720–1680 cm^{-1} is implied of carbonyl groups, vO–H stretching at 1380 cm^{-1} of the alcoholic group and vC–O stretching at 1260–1100 cm^{-1} is corresponding to single C–O groups. Also, symmetric C-H stretches (CH_3) at 2883 cm^{-1} [21-23].

The X-ray spectrum was measured to show the crystal structure of the graphite before and after the reaction, as shown in Fig. 4, which shows the X-ray spectrum of the graphite before interaction and the graphite with nickel sulfate before purification and nanographite, where the peak appears at 26.557° and other weak peaks belong to the hexagonal shape of the graphite. After the heating treatment of graphite-saturated nickel sulfate before purification, the peaks are similar to graphite, which indicates the process is incomplete to form nanographite. But a change is observed in the intensity of the diffraction angles at 26.557 was high for the graphite and the angle is displaced to 26.525 with low intensity where the high intensity is attributed to the crystallized shape of the graphite, while when the intensity of the peak is reduced, the crystallization is less as a result of the platelets crashing into singular plates. The carbon DB card number 9012230 (space group: P63mc) provided a satisfactory identification and description of the positions and intensities of the diffraction peaks. The appearance of a weak angle in the position of 2 theta=10.7 belongs to graphite

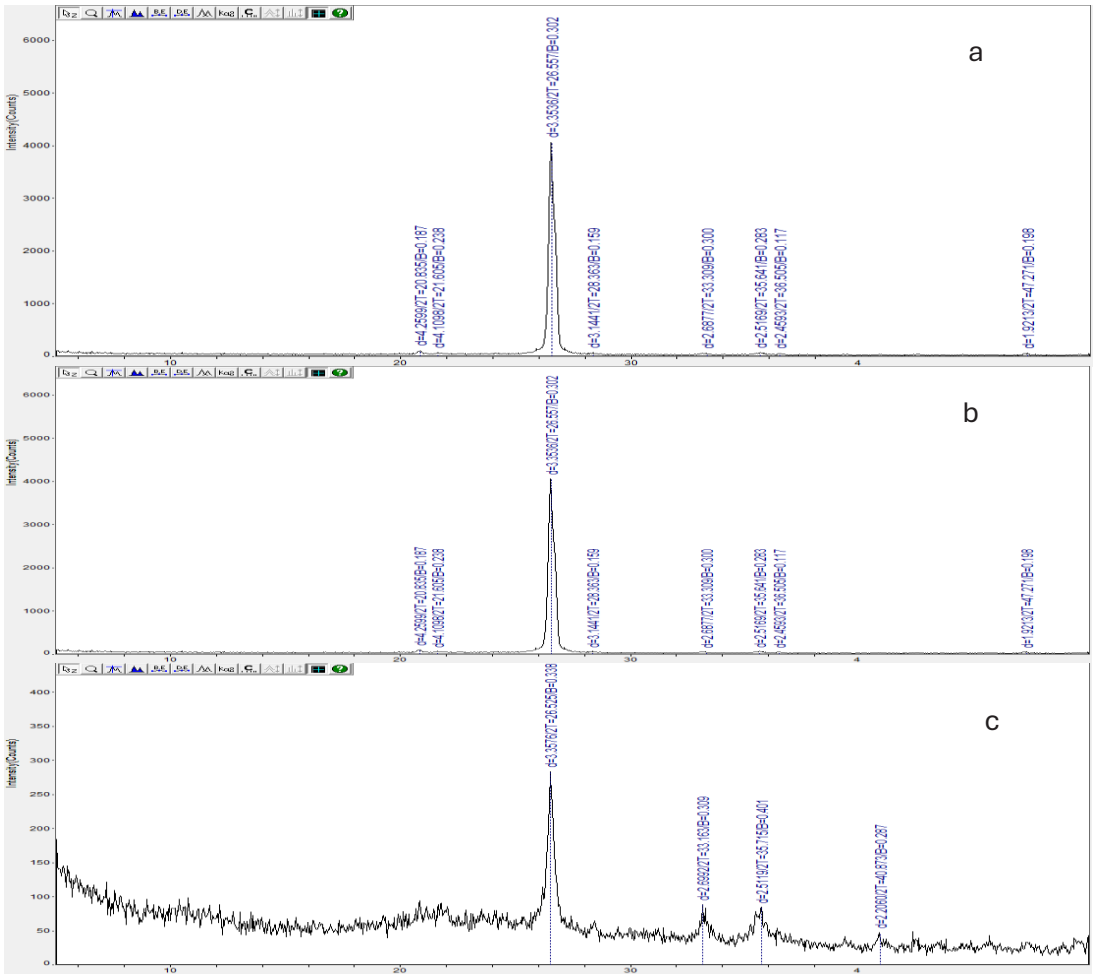

Fig. 4. XRD pattern of graphite (a), treated graphite with nickel sulfate (b), and purified nanographite (c).

oxide and the stacked layer height is 5 nm at 2theta=21.7 is wide and weak, but it belongs to the amorphous phase of nanographite. Also, Bragg's equation (1) was used to determine the separation between the graphene layers in nanographite and graphite oxide. The average height of stacking layers (H) was calculated using Sherrer's equation (2). Additionally, formula (3) was used to assess the number of layers in nanographite. Table 1 displays the results that were obtained:

$$d_{002} = \lambda / 2\sin(\theta) \quad (1)$$

$$H = K\lambda / \beta\cos(\theta) \quad (2)$$

$$n = H/d_{002} \quad (3)$$

where d_{002} representing the distance between graphene layers, λ representing the X-ray wavelength of 0.15406 nm, θ representing the diffraction reflex location, H representing the average height of the crystallite, K representing the form factor (for graphite materials, K = 0.94), and β representing the full width at half-maximum of the diffraction reflex [24].

SEM test is shown in Fig. 5, where the images in different scales and the nanographite like flakes. The procedure deals with the exfoliating of micro graphite with intercalation of nickel sulfate in the inner space of graphite then heat treatment makes the layers disorder easily. This procedure can produce nanographite as a flake. The dimension of the flake (Fig. 5a and b) is measured according to the scale bar of the SEM image by using (the imagej program) with different lengths of 6000-12000 nm and the width was 2000-5000 nm. Also,

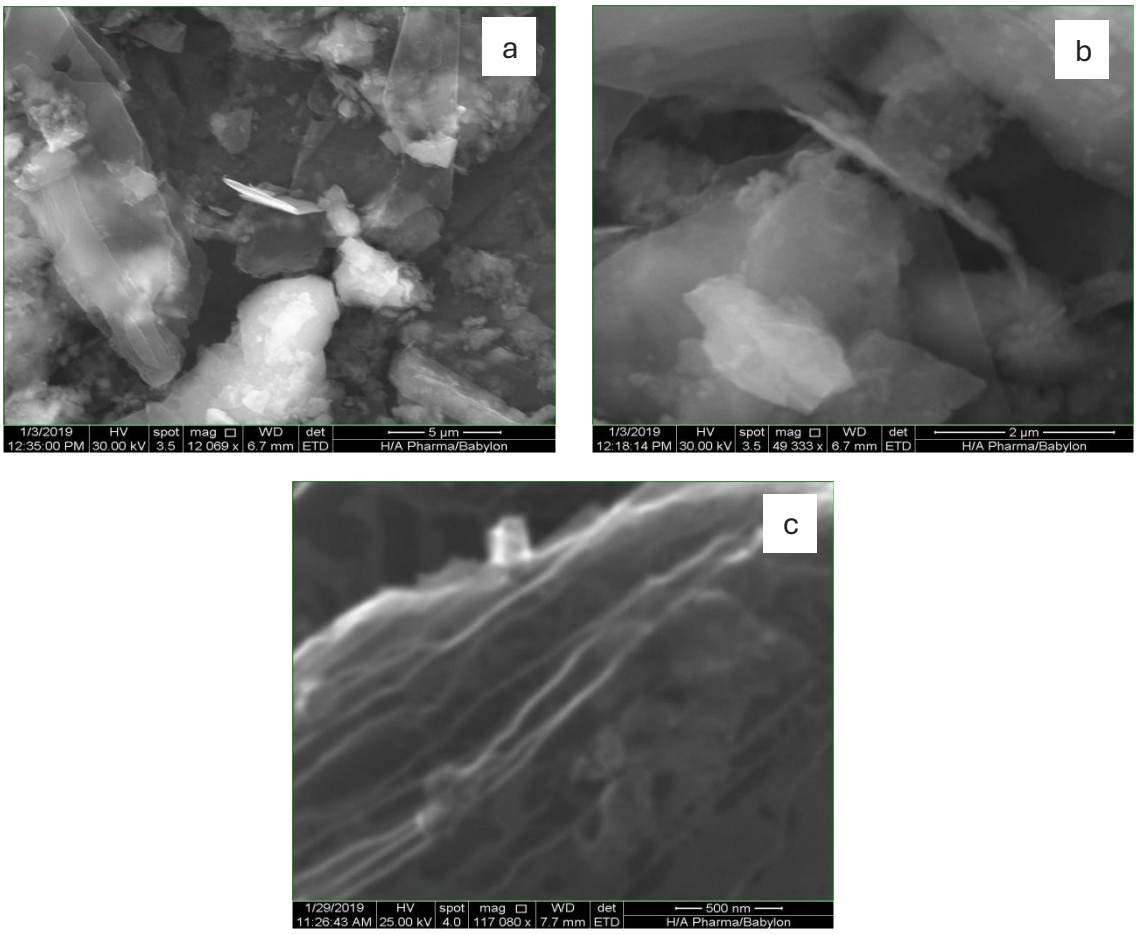

Fig. 5. SEM image of nanographite.

the sample contains fine particles and these are confirmed by XRD according to 2theta=21. In Fig. 5c the image shows the interlayers of each flake, where the thickness of each sheet is 40 nm and this height is near the calculated from XRD parameters as in Table 1. The layers of graphite are displaced from each other, which appeared in Fig. 5c, and the metal exfoliating is the determining condition of nanographite.

Photocatalytic activity of nanosheets is the next level of pollutant remediation and occupies wide application because of the structure of two dimensions with oxygen functionalized groups, high surface area, and the active site is very huge; giving a fast surface charge transfer. These features give nanosheets (like graphene oxide) wide space in reaction and high adsorption of cationic dye molecules and negatively charged oxygen-containing functional goups [25-26]. Also, the oxygen contents in graphene oxide change the polarity from hydrophobic to hydrophilic which would be a good compatibility with photocatalysis applications. The photocatalysis of prepared nanographite by exfoliating is examined by photodegradation of CV solution. The nanographite acts as a semiconductor that enhances charge transfer by the absorption of UV light to give electron-hole pairs these pairs are photoinduced generation and tend to migrate to the surface. These pairs act as oxidizing and reducing sites that can be consumed for CV degradation that is adsorbed on the surface [27].

The photocatalytic degradation of CV dye using synthesized nanographite was accomplished in an aqueous solution with UV illumination. The reactor uses a dipped UV lamp with cooling by

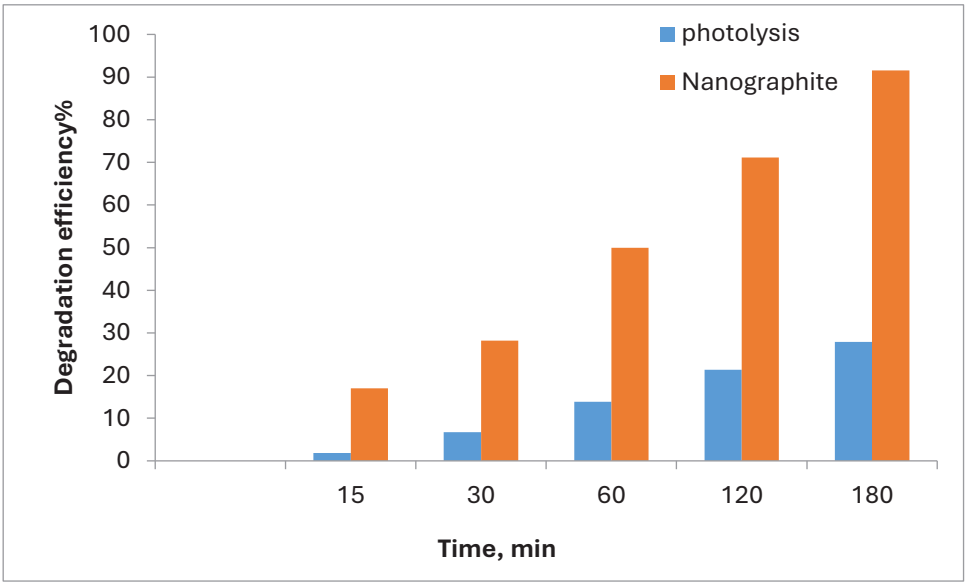

Fig. 6. Photodegradation efficiency of CV dye solution in the

Table 1. the structural parameters of nanographite according to XRD calculation.

2Theta	d, Å	FWHM	H, nm	n
10.729	8.2391	1.541	5	6-7
26.530	3.3570	0.371	22	65-66
33.179	2.6979	0.409	20	74-75
35.669	2.5151	0.779	10	39-40

a water circulator. The preliminary experiment was a mixing of nanographite with 10 ppm of CV dye solution and samples collected for 3 h of the reaction time with illumination. The monitoring of CV vanishing depended on 590 nm as the maiximum wavelength to evaluate the degradation process in all solutions. The degradation of CV according the color is noticed that as reaction time proceeded, the absorbance was decreased. This process needs a catalyst and UV illumination in the presence of oxygen. This result revealed that nanographite has the ability of the photodegradation of CV dye solution. In Fig. 6, the absorbance of CV was decreased as the time of reaction increased, where the photodegradation needed 3 h to reach 90%, while in photolysis the degradation efficiency was 27.9%. The presence of the photocatalyst makes the degradation of CV more active and works as a semiconductor that absorbs light and the degradation is effective in comparison with the degradation without nanographite. In the present results, the synthesized graphite nanosheets are active photocatalyst and can respond to UV light irradiation and succeed in the conversion of light energy into a chemical reaction for CV degradation [28-29].

The effect of nanographite amount used in photodegradation was studied as the weight of the catalyst in the slurry significantly changed the rate of reaction. In this manner, the changing of nanographite weight was studied in the range of 10-40 mg/100 ml of CV solution. In these circumstances the concentration of CV dye was 10 ppm and the pH=7 and ambient temperature. As shown in Fig. 7, The degradation efficiency nanographite was high relatively at 20 mg/100 mL, while the degradation efficiency was low in the case of lower or upper than 20 mg/100 mL. This means the degradation was optimized in the direction of catalyst dose, where the degradation is increased as the weight of the catalyst increases. This is due to the dependency of degradation on the number of active sites that are affected by the amount of catalyst. But in the case of increasing the amount of catalyst the degradation efficiency was decreased. The large dose of a catalyst makes an inner filter prevent light from penetrating inside the slurry. This leads to more inactive sites and leads to low degradation [30-31]. In Fig. 7, the weight of nanographite was studied and showed high degradation efficiency in the case of 20 mg/mL.

The effect of the oxidizing agent on the photodegradation of CV was studied, where the common agent is hydrogen peroxide. This oxidized compound is considered the excellent oxidizing species that is supplied for photodegradation. Hydrogen peroxide was added to the suspension of nanographite in the CV solution, which is the more effective procedure for studying the action

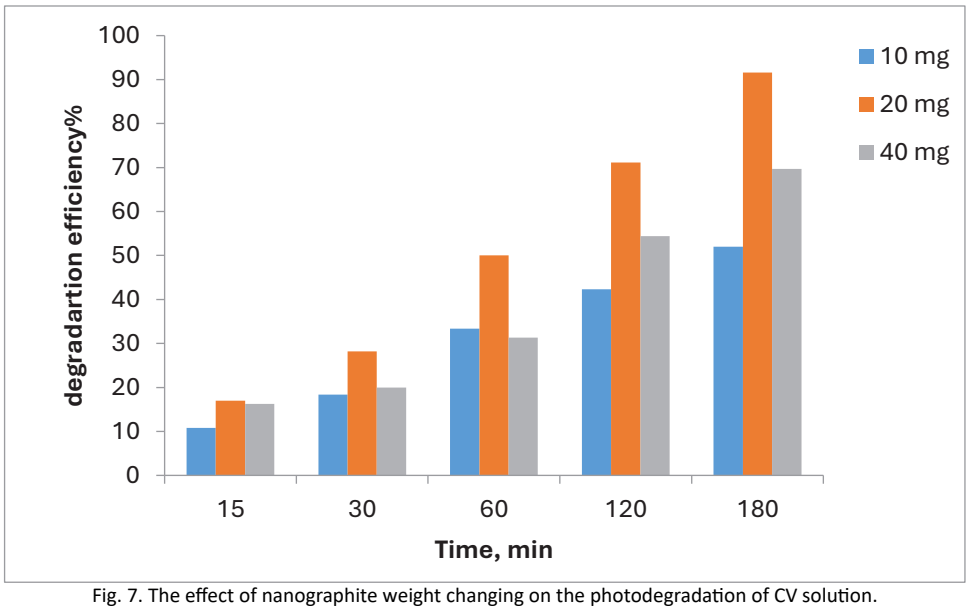

Fig. 7. The effect of nanographite weight changing on the photodegradation of CV solution.

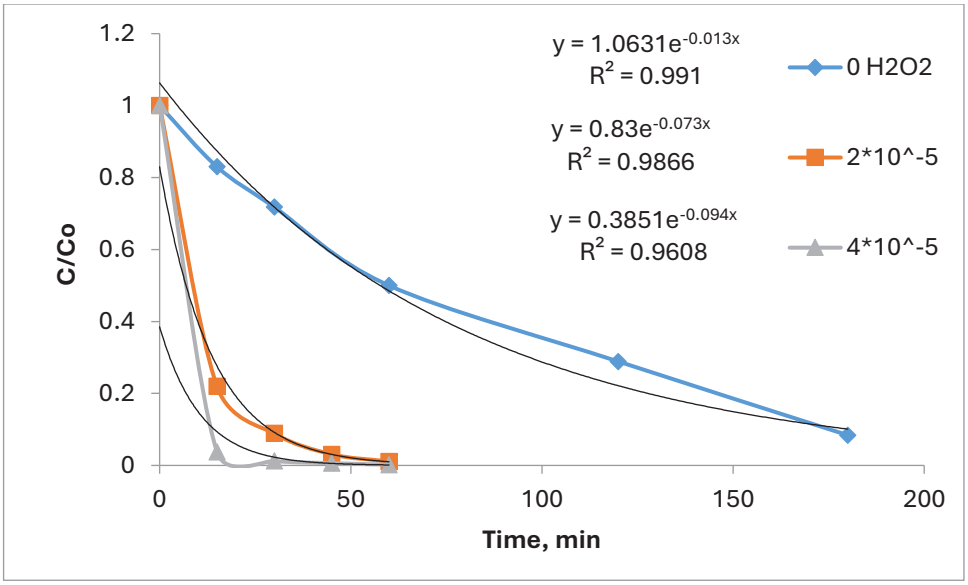

Fig. 8. The relationship between C/C_0 of CV dye with time before and after hydrogen peroxide addition.

of photodegradation[32]. Hydrogen peroxide work to draw electron away from the excited conduction band making more separation of charges on the surface of the photocatalyst. Also, hydrogen peroxide generates the reactive radical species as in the following equations:

$$H_2O_2+e^- \rightarrow OH^- + OH^{\cdot}$$

$$H_2O_2+O^-_2 \rightarrow OH^- + OH^{\cdot} + O_2$$

The action of hydrogen peroxide was very effective in comparison to the nanographite alone. The concentration of hydrogen peroxide was critical, where it was $2*10^{-5}$ and $4*10^{-5}$ M. In the presence of hydrogen peroxide, the photodegradation effectively changed with very interesting high degradation efficiency and it was 98.9% and 99.8% respectively, and the reaction lasted only 1h, while it lasted 3h in the case of nanographite alone. It is worth noting that, in the case of hydrogen peroxide at the concentration of $4*10^{-5}$ M needs only 15 min to vanish the CV dye solution color and the degradation efficiency was 96%. In Fig. 8, the relationship of C/C_0 with the reaction time of CV degradation by using nanographite and hydrogen peroxide. The exponential plot of C/C_0 with time was obtained and the trend line of this curve is the rate constant which was 0.013, 0.073, and 0.094 min^{-1} for nanographite, $2*10^{-5,}$ and $4*10^{-5}$ M of hydrogen peroxide respectively. This action and high photodegradation can be explained by the formation of transition transition-activated complex that makes the electron density transfer from π orbital of nanographite to the hydrogen peroxide leading to a high decomposion process [33]. These nanosheets can generate the photoreactive species like O_2^- and $^{\cdot}OH$. These species have very strong oxidation action to make the CV more degradable. The efficiency of CV dye degradation by nanographite may be attributed to the high dispersity in aqueous solution, and the process leads to the ease of protons reaching the carbon atoms on the sheets. This made of H_2O_2 rapidly transforms to $^{\cdot}OH$ and this species has a very impact on oxidation during the photocatalytic reaction [34].

CONCLUSION

Nanographite can be exfoliated by nickel sulfate saturation and heating at 500 c. The process yielded oxidized nanographite and brown material dispersed in water. The change in UV-vis and FTIR analysis in nanographite after exfoliating is clear and shows the successful method of preparation. XRD analysis revealed the transformation of bulk graphite to low-intensity diffraction peaks. Nanographite has the ability for photodegradation of CV dye solution with a low and optimum loading dose (0.02 gm/100 ml). CV degradation was

affected by the addition of hydrogen peroxide, where the time without it needed 180 min for degradation of CV dye, but in the presence of it lasted only 15 min with a degradation efficiency of 96%.

CONFLICT OF INTEREST

The authors declare that there is no conflict of interest regarding the publication of this manuscript.

REFERENCES

1. Vaughan DJ. J. W. Anthony, R. A. Bideaux, K. W. Bladh, and M. C. Nichols, Handbook of Mineralogy: Volume I; Elements, Sulfides, Sulfosalts. Tucson, Arizona (Mineral Data Publishing), 1990. viii + 588 pp. Price $82.50 + $5.00 shipping and handling. Mineralogical Magazine. 1991;55(378):146-147.
2. Pierson HO. Molded Graphite: Processing, Properties, and Applications. Handbook of Carbon, Graphite, Diamonds and Fullerenes: Elsevier; 1993. p. 87-121.
3. Zheng W, Wong S-C. Electrical conductivity and dielectric properties of PMMA/expanded graphite composites. Composites Science and Technology. 2003;63(2):225-235.
4. Hardy GF. A review of: "DEVELOPMENTS IN ADHESIVES-2, edited by A. J. Kinloch. Applied Science Publishers, London and Englewood, N.J., 1981, 419 pp. ($68.00).". The Journal of Adhesion. 1982;14(2):175-177.
5. Zheng Z, Zhang J, Huang JY. Observations of microstructure and reflectivity of coal graphites for two locations in China. International Journal of Coal Geology. 1996;30(4):277-284.
6. Bliss JD. Industrial minerals deposit models; grade and tonnage models. Open-File Report: US Geological Survey; 1992.
7. Zhu Y, Murali S, Cai W, Li X, Suk JW, Potts JR, et al. Graphene and Graphene Oxide: Synthesis, Properties, and Applications. Adv Mater. 2010;22(35):3906-3924.
8. Hummers WS, Offeman RE. Preparation of Graphitic Oxide. Journal of the American Chemical Society. 1958;80(6):1339-1339.
9. Chen J, Yao B, Li C, Shi G. An improved Hummers method for eco-friendly synthesis of graphene oxide. Carbon. 2013;64:225-229.
10. Stankovich S, Dikin DA, Piner RD, Kohlhaas KA, Kleinhammes A, Jia Y, et al. Synthesis of graphene-based nanosheets via chemical reduction of exfoliated graphite oxide. Carbon. 2007;45(7):1558-1565.
11. Wang Z, Zhou X, Zhang J, Boey F, Zhang H. Direct Electrochemical Reduction of Single-Layer Graphene Oxide and Subsequent Functionalization with Glucose Oxidase. The Journal of Physical Chemistry C. 2009;113(32):14071-14075.
12. Pumera M. Graphene-based nanomaterials for energy storage. Energy Environ Sci. 2011;4(3):668-674.
13. Li X, Cai W, An J, Kim S, Nah J, Yang D, et al. Large-Area Synthesis of High-Quality and Uniform Graphene Films on Copper Foils. Science. 2009;324(5932):1312-1314.
14. Berger C, Song Z, Li T, Li X, Ogbazghi AY, Feng R, et al. Ultrathin Epitaxial Graphite: 2D Electron Gas Properties and a Route toward Graphene-based Nanoelectronics. The Journal of Physical Chemistry B. 2004;108(52):19912-19916.
15. Rollings E, Gweon GH, Zhou SY, Mun BS, McChesney JL, Hussain BS, et al. Synthesis and characterization of atomically thin graphite films on a silicon carbide substrate. Journal of Physics and Chemistry of Solids. 2006;67(9-10):2172-2177.
16. Schniepp HC, Li J-L, McAllister MJ, Sai H, Herrera-Alonso M, Adamson DH, et al. Functionalized Single Graphene Sheets Derived from Splitting Graphite Oxide. The Journal of Physical Chemistry B. 2006;110(17):8535-8539.
17. Stankovich S, Piner RD, Chen X, Wu N, Nguyen ST, Ruoff RS. Stable aqueous dispersions of graphitic nanoplatelets via the reduction of exfoliated graphite oxide in the presence of poly(sodium 4-styrenesulfonate). J Mater Chem. 2006;16(2):155-158.
18. Kyriakos P, Hristoforou E, Belessiotis GV. Graphitic Carbon Nitride ($g\text{-}C_3N_4$) in Photocatalytic Hydrogen Production: Critical Overview and Recent Advances. Energies. 2024;17(13):3159.
19. Purba FJ, Sitorus Z, Tarigan K, Siregar N. Enhanced Photocatalytic Activity of Cu_2O/ZnO/GO Nanocomposites on the Methylene Blue Degradation. Baghdad Science Journal. 2023.
20. Peyvandi A, Soroushian P, Abdol N, Balachandra AM. Surface-modified graphite nanomaterials for improved reinforcement efficiency in cementitious paste. Carbon. 2013;63:175-186.
21. Abdullaeva Z, Kelgenbaeva Z, Masayuki T, Hirano M, Nagaoka S, Shirosaki T. Graphene Sheets with Modified Surface by Sodium Lauryl Sulfate Surfactant for Biomedical Applications. Graphene. 2016;05(04):155-165.
22. Radoń A, Łukowiec D. Structure of nanographite synthesised by electrochemical oxidation and exfoliation of polycrystalline graphite. Micro and Nano Letters. 2017;12(12):955-959.
23. Zhao XM, Malik MJ. Electrochemical Fabrication of Graphite Oxide Nanosheets with Stable Photoluminescence and Their Photocatalytic Performance in Visible Light. Asian J Chem. 2013;25(12):6877-6880.
24. Khezami L, Ben Aissa MA, Modwi A, Ismail M, Guesmi A, Algethami FK, et al. Harmonizing the photocatalytic activity of $g\text{-}C_3N_4$ nanosheets by ZrO_2 stuffing: From fabrication to experimental study for the wastewater treatment. Biochem Eng J. 2022;182:108411.
25. Thangavel S, Venugopal G. Understanding the adsorption property of graphene-oxide with different degrees of oxidation levels. Powder Technol. 2014;257:141-148.
26. Bissessur R, Scully S. Intercalation of solid polymer electrolytes into graphite oxide. Solid State Ionics. 2007;178(11-12):877-882.
27. Putri LK, Tan L-L, Ong W-J, Chang WS, Chai S-P. Graphene oxide: Exploiting its unique properties toward visible-light-driven photocatalysis. Applied Materials Today. 2016;4:9-16.
28. Hsu H-C, Shown I, Wei H-Y, Chang Y-C, Du H-Y, Lin Y-G, et al. Graphene oxide as a promising photocatalyst for CO_2 to methanol conversion. Nanoscale. 2013;5(1):262-268.
29. Matsumoto Y, Koinuma M, Ida S, Hayami S, Taniguchi T, Hatakeyama K, et al. Photoreaction of Graphene Oxide Nanosheets in Water. The Journal of Physical Chemistry C. 2011;115(39):19280-19286.
30. Lonkar SP, Pillai V, Abdala A. Solvent-free synthesis of ZnO-graphene nanocomposite with superior photocatalytic activity. Appl Surf Sci. 2019;465:1107-1113.
31. Vaiano V, Matarangolo M, Murcia JJ, Rojas H, Navío JA, Hidalgo MC. Enhanced photocatalytic removal of phenol from aqueous solutions using ZnO modified with Ag. Applied Catalysis B: Environmental. 2018;225:197-206.
32. Wahab AK, Nadeem MA, Idriss H. Hydrogen Production During Ethylene Glycol Photoreactions Over Ag-Pd/TiO_2 at Different Partial Pressures of Oxygen. Frontiers in Chemistry. 2019;7.
33. Lapko VF, Gerasimyuk IP, Kuts' VS, Tarasenko YA. The activation characteristics of the decomposition of H_2O_2 on palladium-carbon catalysts. Russian Journal of Physical Chemistry A. 2010;84(6):934-940.
34. Three-Dimensional Porous Aerogel Constructed by gC3N4 and Graphene Oxide Nanosheets with Excellent Visible-Light Photocatalytic Performance. American Chemical Society (ACS).